Chemical Geology 396 (2015) 228–238

Contents lists available at ScienceDirect

Chemical Geology

journal homepage: www.elsevier.com/locate/chemgeo

Seasonal release of anoxic geothermal meltwater from the Katla volcanic system at Sólheimajökull, Iceland

Peter M. Wynn [a,*], David J. Morrell [a], Hugh Tuffen [a], Philip Barker [a], Fiona S. Tweed [b], Rebecca Burns [a]

[a] Lancaster Environment Centre, University of Lancaster, Lancaster LA1 4YQ, UK
[b] Geography, Staffordshire University, Leek Road, Stoke-on-Trent, Staffordshire ST4 2DF, UK

ARTICLE INFO

Article history:
Received 30 September 2014
Received in revised form 23 December 2014
Accepted 25 December 2014
Available online 4 January 2015

Editor: Michael E. Böttcher

Keywords:
Iceland
Mýrdalsjökull
Sólheimajökull
Geothermal water
Glacial hydrochemistry
Sulphate isotopes

ABSTRACT

Understanding patterns of geothermal and volcanic activity at many of Iceland's most active volcanic systems is hampered by thick overlying ice, which prevents direct observation and complicates interpretation of geophysical signals. Katla is a prime example, being a large and restless volcanic system covered by the 740 m thick Mýrdalsjökull ice cap, whose eruptions have triggered some of the most powerful known meltwater floods in historical times. To shed new light on geothermal and subglacial hydrological processes at Katla, we have determined the sulphate isotopic composition of a series of glacial meltwater samples discharged from Sólheimajökull, a valley glacier of Mýrdalsjökull, between 2009 and 2012. Dual isotopic analysis of $\delta^{34}S$ and $\delta^{18}O$ in dissolved sulphate allows identification of source mixing processes and chemical evolution during subglacial meltwater transport. Strikingly, meltwater $\delta^{18}O_{SO_4}$ signatures indicate redox conditions at the glacier bed, which are inverse to those normally encountered at Arctic and Alpine glaciers. Discharge of reduced, anoxic meltwater in summer, rather than winter, points towards seasonal release of geothermally derived volatile gases. We attribute this to headward expansion of the channelized subglacial drainage system during the summer melt season, accessing key areas of geothermal activity within the Katla caldera. Volatile release may be further enhanced by unloading of overburden pressure due to snowpack melting in the summer season. In winter, restriction of subglacial channels to lower elevations effectively seals geothermal fluids and dissolved gases beneath the ice cap, with only sporadic release permitted by periodic increases in subglacial water pressure. When the subglacial drainage configuration permits access to key geothermal areas, sulphate isotopic signatures thereby form sensitive indicators of geothermal activity occurring deep beneath the Mýrdalsjökull ice cap.

1. Introduction

Glacial meltwater hydrochemistry is typically used as a fingerprinting technique for deciphering physical, chemical and biological processes occurring deep beneath ice masses (e.g. Tranter et al., 1993, 1997; Hodson et al., 2005; Galeczka et al., 2014). Such information is particularly significant in the context of glaciated volcanoes, where ice cover complicates interpretation of geophysical signals, making eruptive events difficult to forecast or identify (Guðmundsson et al., 2008). Melting of ice in glaciated volcanic systems may stimulate eruptive and geothermal activity (e.g. Pagli and Sigmundsson, 2008; Tuffen, 2010), which in turn can destabilise ice bodies (Bell, 2008), creating positive feedback that may have major environmental implications (Huybers and Langmuir, 2009). Several studies have addressed the discharge and geochemical composition of episodic flood waters generated through subglacial volcanic eruptions (e.g. Elefsen et al., 2002; Galeczka et al., 2014; Gíslason et al., 2002), although few have used sensitive geochemical indicators to monitor the continual evolution of ice-capped geothermal systems (Kristmannsdóttir et al., 2002). Here, we evaluate the incidence of subglacial geothermal activity at Sólheimajökull, Iceland, an outlet glacier from the Mýrdalsjökull ice cap, which conveys large quantities of volatiles dissolved in meltwater outlet streams. The Sólheimajökull subglacial drainage system conveys volatile species derived from the ice-covered Katla caldera on the Mýrdalsjökull–Katla system, with the frequent smell of hydrogen sulphide emanating from the meltwater streams providing a strong indication of persistent subglacial geothermal activity (Björnsson et al., 2000). Existing research has documented the background chemistry in bulk meltwater outputs from the catchment and tentatively attributed these to variations in the strength of the Katla geothermal field (Sigvaldason, 1963; Lawler et al., 1996). However, the drivers of geothermal activity, and whether any associated chemical signal could be used reliably to understand processes in the subglacial geothermal system at Katla, remain poorly understood. Stable isotopes allow fingerprinting of subglacial chemical sources, their mixing and chemical evolution during meltwater transport. The rapid oxidation of reduced sulphurous gases to sulphate, which is subsequently relatively stable in solution, makes the dual isotopic analysis of sulphate an attractive contender as an indicator of subglacial geothermal activity. This paper aims to i) identify the sources and

* Corresponding author. Tel.: +44 1524 510235.
E-mail address: p.wynn@lancaster.ac.uk (P.M. Wynn).

http://dx.doi.org/10.1016/j.chemgeo.2014.12.026
0009-2541/

biogeochemical cycling of sulphur beneath the Mýrdalsjökull ice cap, ii) explain seasonal variations in redox status at the glacier bed, and iii) evaluate the use of sulphur isotopes as indicators of subglacial geothermal activity. We begin by briefly reviewing the nature of sulphate acquisition and isotopic signatures within glaciated catchments to provide context to the study.

2. Sulphur acquisition and isotopic signatures within glaciated catchments

Sources of sulphur within glaciated catchments are predominantly restricted to atmospheric deposition and release from catchment geology. Atmospheric sulphur deposition is composed of marine aerosol and industrial pollution, with minor components from volcanic outgassing and continental biogenic emissions. Oxidation in the atmosphere to sulphate and subsequent deposition as rain/snowfall creates a supraglacial sulphate input to the glacier which varies in concentration and isotopic composition depending upon the dominance of each of the above sources. Sulphur isotopic values of each of the sources range between marine aerosol, which varies little from +21‰ (Rees et al., 1978) and continental biogenic emissions that form a light isotopic end member ranging from approximately 0 to −30‰ (Nielson, 1974). Volcanic aerosol emissions approximate 0‰ (Nielsen et al., 1991) and the release of sulphur gases from combustion of fossil fuels depends upon the sulphur isotopic composition of the source materials which has the capability of stretching over the whole range of values given above (see inventory in Newman et al., 1991; Nielson, 1974). The isotopic signature of precipitation thereby reflects this mixed composition of sulphur inputs. For $\delta^{34}S_{SO_4}$ found within European precipitation (including snowfall) the typical range is between −3 and +9‰ reflecting a high proportion of industrial pollution (Mayer, 1998); for precipitation over mid-latitude sites, the range resides between −2.5 and +13.5‰ (Jenkins and Bao, 2006), whilst $\delta^{34}S_{SO_4}$ extracted from shallow ice cores in central Antarctica ranges between +9.3 to +18.1‰ (Patris et al., 2000) and +14.5 to +15.0‰ (Jonsell et al., 2005) reflecting a dominance of marine, and volcanic input in the absence of industrial pollution.

Catchment geology contributes to the sulphur load in glacial meltwaters through release of sulphur from geothermal activity and weathering of bedrock. Release of sulphur species from geothermal areas is documented to have a downstream impact on the load and isotopic composition of sulphate leaving glaciated catchments, dependent upon the strength of the geothermal field and the dissolution of volatile sulphur species into ground waters (e.g. Gíslason et al., 2002; Robinson et al., 2009). Bedrocks contain sulphur usually in the form of pyrite, gypsum, or secondary mineral precipitates. Studies of bedrock sulphur isotope composition from volcanic rocks within Iceland range from −2 to +0.4‰ for basalts, and up to +4.2‰ for acidic volcanic rocks (Torssander, 1989). $\delta^{34}S$ values of pyrite from rhyolite clasts at Skeiðarársandur range between −1.2 and +2.6‰ (Robinson et al., 2009) and $\delta^{34}S$ values of lava incrustations (sublimates deposited in solidifying lavas) reflect closely the isotopic signature of host basalts and precursor volcanic gas species (Torssander, 1988). Acquisition of sulphur by bedrock weathering beneath a glacier proceeds via oxidation and dissolution reactions. Both of these reactions are largely dependent upon rock–water contact time and availability of dissolved gases, governed according to the subglacial or proglacial environment of solute acquisition and associated hydrological characteristics (e.g. Bottrell and Tranter, 2002; Wynn et al., 2006; Wadham et al., 2007).

Different types of subglacial drainage system are widely held to exist beneath glaciers and ice sheets, their characteristics dependent on meltwater discharge, temperature distribution at the ice–bed interface and the topography, permeability and rigidity of the glacier bed. Within temperate glacial systems such as those considered as a part of this paper, research recognises two main types of subglacial drainage; firstly discrete systems in which water is confined to a few channels or conduits, and secondly, distributed systems in which water is stored and transported over all or large parts of the glacier bed (e.g. Kamb, 1987; Lliboutry, 1968, 1979; Walder, 1986). Discrete systems are efficient transporters of meltwater exhibiting rapid flow through a well-connected conduit system; in contrast, distributed systems are inefficient, with meltwater flowing slowly through poorly-connected networks. Distributed systems often take the form of linked cavity drainage networks, in which cavities permit temporary water storage and narrow connections or orifices link the cavities together. As subglacial discharge increases, melting of ice from the roof of the cavities offsets some of the ice pressure that would cause cavity closure and large low-pressure cavities effectively capture drainage from small high-pressure cavities, enlarging as they do so. Eventually the linked cavity drainage network becomes unstable at high meltwater discharges and the system switches to a discrete, efficient system (Fountain and Walder, 1998).

Both discrete and distributed drainage systems (termed 'quick flow' and 'delayed flow' respectively according to the residence time of meltwater at the bed within each) are not mutually exclusive, but compete on an annual basis such that the quick flow channelized system demonstrates headward expansion during the melt season and the delayed flow linked cavity system becomes spatially restricted to areas where a deep snowpack minimises the flux of water to the glacier bed. During periods of minimal melting, channelized systems close due to ice deformation, although cavity networks remain open and demonstrate spatial expansion due to a reliance on ice dynamics for cavity formation (Fountain and Walder, 1998). On temperate Icelandic glacial systems, where year-round melting usually persists in the lower reaches of the glacier, discrete channelized systems remain a permanent feature. Changes to the extent of the channelized network are determined through seasonal water flux to the glacier bed and mirror changes in the extent of the distributed system (Björnsson, 1988; Flowers, et al., 2003). This switch in the hydrology is mimicked through a 'switch' in the chemistry, associated with the degree of rock–water contact and availability of atmospheric gases afforded by each system. Distributed systems with extensive rock–water contact drive enhanced solute acquisition. The limited supply of atmospheric gases to the glacier bed determines the suite of available reaction mechanisms with many reactions in distributed systems occurring under conditions of low redox status (Wynn et al., 2006). Quick flow systems transit the subglacial environment with such rapidity that the degree of rock–water contact is a limiting factor on solute acquisition from bedrock weathering (Tranter et al., 1993). Acquisition of solutes from bedrock weathering continues through the proglacial zone through reaction with suspended sediments (e.g. Brown et al., 1994; Fairchild et al., 1999), weathering of near surface moraine and from contributing groundwaters (Wadham et al., 2007; Robinson et al., 2009), and re-dissolution of gypsum and other secondary mineral precipitates (Cooper et al., 2002).

Where ambient environmental conditions are fully oxidising and the supply of atmospheric gases does not represent a limiting factor, there is very limited fractionation of sulphur isotopes during oxidative weathering (Taylor et al., 1984). Dissolution of secondary mineral precipitates and volatile geothermal gases is also documented to incur minimal isotopic fractionation (Ohmoto and Rye, 1979). The dissolved sulphate load in glacial meltwaters thereby retains an isotopic signature that directly reflects the isotopic composition of the geologic parent materials. However, under strongly reducing conditions, dissolved sulphate can be microbially reduced to produce sulphide, leaving a residual pool of dissolved sulphate enriched in ^{34}S and ^{18}O (eg. Spence et al., 2001; Strebel et al., 1990). Under anoxic conditions beneath glaciers which are closed to the external environment, a positive relationship between $\delta^{34}S_{SO_4}$ and $\delta^{18}O_{SO_4}$ in the residual dissolved sulphate pool is indicative of microbial sulphate reduction (Wadham et al., 2004). At redox conditions of intermediate status, representing areas of the subglacial system that are poorly connected to the atmosphere, oxidising agents other than atmospheric oxygen are used to drive oxidation weathering, mediated through microbiological activity

(e.g. Bottrell and Tranter, 2002). During this process, the sulphur isotopic composition of the source bedrock is preserved in the product sulphate, although oxygen source mixing and isotopic exchange between water and sulphur intermediate species leave a distinctive $\delta^{18}O_{SO_4}$ signature serving as an important indicator of redox status.

Under atmospheric conditions, the oxidation of sulphide to sulphate is dependent upon obtaining an oxygen source from both atmospheric O_2 and H_2O (Eq. (1)).

$$4FeS_{2(s)} + 15O_{2(aq)} + 14H_2O_{(l)} \rightarrow 16H^{+}_{(aq)} + 4Fe(OH)_{3(s)} + 8SO_{4(aq)}^{2-}. \quad (1)$$

However, if atmospheric oxygen is not available, the reaction can still proceed, albeit through microbial mediation under reducing conditions, using water as the sole oxygen provider (Eq. (2)).

$$FeS_2 + 14Fe^{3+} + 8H_2O \rightarrow 2SO_4^{2-} + 15Fe^{2+} + 16H^{+}. \quad 2$$

Due to the large isotopic difference between oxygen sources used during the process of oxidation ($H_2O = -9.66‰$ (average value of Sólheimajökull melt water $\delta^{18}O_{H_2O}$); atmospheric $O_2 = +23.88‰$ (Barkan and Lus, 2005)), the varying proportion in which they are incorporated into the sulphate molecule can inform about the environmental redox status at the point of formation.

The instability of intermediate reaction products during the formation of sulphate means up to three of the four constituent oxygen atoms undergo rapid equilibration with the surrounding water (Holt and Kumar, 1991). At low temperature and pH, the final oxygen incorporated into the sulphate molecule is stable and thereby indicative of source (Lloyd, 1968). Sulphate molecules, which contain at least 25% oxygen obtained from an atmospheric source, are thereby indicative of a subglacial drainage system which is connected to the atmosphere. For those sulphate molecules with >75% oxygen obtained from H_2O, it can be assumed that these were formed under conditions of low redox status through microbially-mediated reaction mechanisms utilising Fe^{3+} as an oxidising agent. A threshold isotopic value can be calculated to express this classification of sulphate molecules according to the ambient redox conditions in their environment of formation (Eq. (3)) (after Bottrell and Tranter, 2002).

$$\delta^{18}O_{threshold} = [(23.88–8.7) \times 0.25] + \left(0.75 \times \delta^{18}O_{H_2O}\right) \quad (3)$$

where +23.88‰ represents the isotopic value of atmospheric oxygen (Barkan and Lus, 2005), which incurs an experimentally determined fractionation of −8.7‰ during incorporation into the sulphate molecule (Lloyd, 1968). Where sulphur intermediate species are a product of this oxidation reaction (eg. elemental sulphur and thiosulphate), bacterial disproportionation reactions can lead to the formation of hydrogen sulphide and/or sulphate (Böttcher et al., 2005). The extent of fractionation associated with disproportionation depends on the presence of either iron or manganese as oxidising agents (Böttcher and Thamdrup, 2001; Böttcher et al., 2001) but may enrich product sulphate in ^{34}S by up to +35‰ and in ^{18}O by up to +21‰ compared to precursor sulphur compounds and water respectively. Repeated cycles of disproportionation and re-oxidation will deplete product sulphides in ^{34}S beyond the envelope of fractionation expected through processes of sulphate reduction alone (Canfield and Thamdrup, 1994).

Glaciers have been observed to fluctuate in subglacial redox status largely according to seasonality. In High Arctic and temperate glacial systems, spring season and early summer subglacial meltwaters suggest low redox status at the bed of the glacier. Full oxygenation returns during times of high summer discharge (Bottrell and Tranter, 2002; Wynn et al., 2006, 2007). Evidence for occasional recurrence of low redox status during the summer season has been attributed to persistence of the distributed drainage system under portions of the glacier and its variable mixing with oxygen saturated quick flow melt waters on a range of timescales (Bottrell and Tranter, 2002; Irvine-Fynn and Hodson, 2010).

Due to the limited isotopic fractionation of geological sulphur species under oxidising conditions and the frequent overlap in isotopic signatures between sulphur released from geothermal sources and those released from mineral sources, the use of sulphate isotopes as indicators of subglacial geothermal processes is still poorly documented and understood. Attribution of any chemical fingerprint to understanding subglacial geothermal processes must rely on being able to deconvolve mixing of sulphur sources, as well as indicate mechanisms of biogeochemical cycling and chemical evolution during transport. Here, we use stable environmental isotopes of $\delta^{34}S_{SO_4}$ and $\delta^{18}O_{SO_4}$ in conjunction with conventional meltwater chemical assays to identify the sources and biogeochemical cycling of sulphur beneath the Mýrdalsjökull ice cap. We implicate the role of subglacial geothermal processes in contributing to the sulphur load and trace the redox evolution of the subglacial hydrological system, which appears to be driven by seasonality in the release of geothermally-produced fluids.

3. Methods

3.1. Site description

The Mýrdalsjökull ice cap covers the Katla volcanic system, which constitutes the central Katla volcano and fissure swarm (Sturkell et al., 2010; Duller et al., 2012). The Katla caldera is 600–750 m deep, and covers an area of 100 km^2. Its rim is breached in three places, which provides outflows of ice to feed the three major outlet glaciers of Sólheimajökull, Kötlujökull and Entujökull (Björnsson et al., 2000; Sturkell et al., 2010). Geothermal activity within the caldera is manifested as several 10–50 m deep ice cauldrons within and at the caldera rim, with a total geothermal output of a few hundred megawatts (Guðmundsson et al., 2007). The drainage divide of Sólheimajökull continues into the southwestern rim of the Katla subglacial caldera, making it possible for volcanically-generated and geothermal ice melt to drain through Sólheimajökull as jökulhlaups (Björnsson et al., 2000; Larsen et al., 2001; Larsen, 2010). Most historic jökulhlaups generated by Katla eruptions have drained through neighbouring Kötlujökull onto Mýrdalssandur to the east; however, some floodwaters generated by the 1860 Katla eruption were routed via Sólheimajökull (Hákonarson, 1860; Björnsson et al., 2000). After this event, the eruption centre moved to the northeast, confining jökulhlaups to Kötlujökull and Mýrdalssandur until 1999, when a volcanically-generated jökulhlaup burst from Sólheimajökull (Roberts et al., 2003; Larsen, 2010; Russell et al., 2010). A number of smaller floods generated by geothermal activity are also known to periodically exit the glacier.

Sólheimajökull itself is 8 km long, non-surging and characterised as a temperate glacier. It supports a maximum ice thickness of 433 m (Mackintosh et al., 2002; Kruger et al., 2010; Russell et al., 2010; Sigurdsson, 2010) and ranges in elevation from 1500 m.a.s.l. down to an over-deepened snout with bed elevation 50 m below sea level (Lawler et al., 1996; Le Heron and Etienne, 2005; Scharrer et al., 2008; Russell et al., 2010). The total area of the glacier is approximately 78 km^2 with the accumulation zone comprising approximately 56% of the total glacier area (Lawler et al., 1996; Roberts et al., 2000; Le Heron and Etienne, 2005). Dynamic advance and retreat cycles are exhibited by the glacier (Schomacker et al., 2012), which are frequently asynchronous with other glaciers along the south coast of Iceland (Dugmore and Sugden, 1991). The proglacial geomorphology reflects this dynamic activity, leaving behind a vivid sequence of moraine assemblages and glaciofluvial outwash features (Staines et al., In Press). The supraglacial drainage across the ice-free area of Sólheimajökull is poorly developed due to extensive crevassing and moulin connectivity to englacial and subglacial hydrological pathways. Proglacial channel morphology has evolved from 2009 to 2012, from a configuration of

two melt water channels conveying water away from the glacier on the western and eastern side of the catchment respectively, to a well-established proglacial lake which has gradually increased in size from 2010 to the present day (Fig. 1). Jökulsá á Sólheimasandi is the bulk meltwater stream leaving the catchment; it has long been known by nearby inhabitants as Fulilaekur or 'stinky river' as the smell of hydrogen sulphide is locally prevalent (Thorarinsson, 1939). Jökulsá á Sólheimasandi carries meltwaters from Sólheimajökull as well as two additional stream inputs originating from outside the catchment. The river Jökulsárgil drains Jökulsárgilsjökull, a small valley glacier flowing from Mýrdalsjökull, and enters the Jökulsá á Sólheimasandi proglacial system (Fig. 1). Fjallgilsá is a small river of non-glacial origin that drains an area of grassland to the south east of Mýrdalsjökull and joins Jökulsá á Sólheimasandi around 2 km down-sandur from the glacier snout. Jökulsá á Sólheimasandi continues to flow in an anastomosing channel, passing under the N1 road bridge 5 km from the glacier front where river stage, EC and water/air temperature are automatically logged by the Icelandic Meteorological Office. The geology of the catchment comprises distinct volcanic bedrock units, each thought to predominantly represent a single eruptive episode. Between each unit, striated erosion surfaces support tillites, fluvioglacial deposits and occasional sub-aerial weathering defining periods of landscape denudation and glacial erosion (Carswell, 1983). A detailed chemostratigraphy of each unit is provided in Carswell (1983), highlighting the dominant basalt lava type found within the majority of units to be classified as a transitional alkalic type. The sulphur content of the rocks within the whole succession has not previously been documented, although the sulphur composition of mixed subglacial till and pyrite-bearing lithologies recently revealed by the receding ice margin are discussed below.

3.2. Field sampling

Field samples were collected over a period of 4 years from 2009 to 2012, comprising two summer and one spring season sampling campaign. A limited number of samples were also collected in the September of each year. The precise time intervals during which sampling was undertaken, the number of samples collected in each sampling interval, and the temporal comparability of sample collection between seasons are detailed within Tables 1 and 2. Sample collection sites remained at consistent locations throughout the four years, as far as the evolving nature of the proglacial system allowed (Fig. 1) and included meltwaters sampled from supraglacial locations, at sites flanking the edges of the proglacial lagoon, subglacial upwellings located at the frontal ice margin, bulk meltwaters located at the outlet of the lagoon and 5 km downstream beneath the N1 road bridge, and streams of external catchment origin. Repeat samples were taken at consistent intervals at each collection site throughout the period of monitoring. At each site, measurements of EC, pH and DO were taken using a handheld multi-parameter WTW 340i combination metre (Wissenschaftlich-Technische Werkstätten GmbH). Water samples were collected and filtered through 0.45 μm cellulose nitrate membrane filters using a handheld Nalgene filter pump. Aliquots were bottled (LDPE Nalgene bottles) without headspace and determination of major ions, cations and trace metals was undertaken within one month of return from the field (only select ions are reported here). Hydrogen sulphide was extracted for isotopic analysis as zinc sulphide, following addition of zinc acetate and collection by filtration (0.45 μm cellulose nitrate membrane filters). For sulphate isotope pre-concentration, 0.5 l of filtered water was loaded onto a 1 ml volume of ion exchange resin immediately after collection (AG2-X8 and 50W-X8 resin for anion and cation removal respectively). Water samples collected for determination of D/O isotopes were bottled unfiltered and without headspace to minimise the fractionating effects of evaporation.

3.3. Laboratory analysis

Laboratory analyses of major anions were determined by ion chromatography (Dionex ICS4000 system). Precision based on repeat analysis of reference standard material of comparable concentration to the samples being analysed was calculated as +/− 5%. Limits of detection were calculated based on blank determinations subjected to the same collection and storage procedure as field samples.

In preparation for analysis of sulphate isotopes, anions were removed from the AG2-X8 resin using aliquots of 1 M ultrapure HCl to a

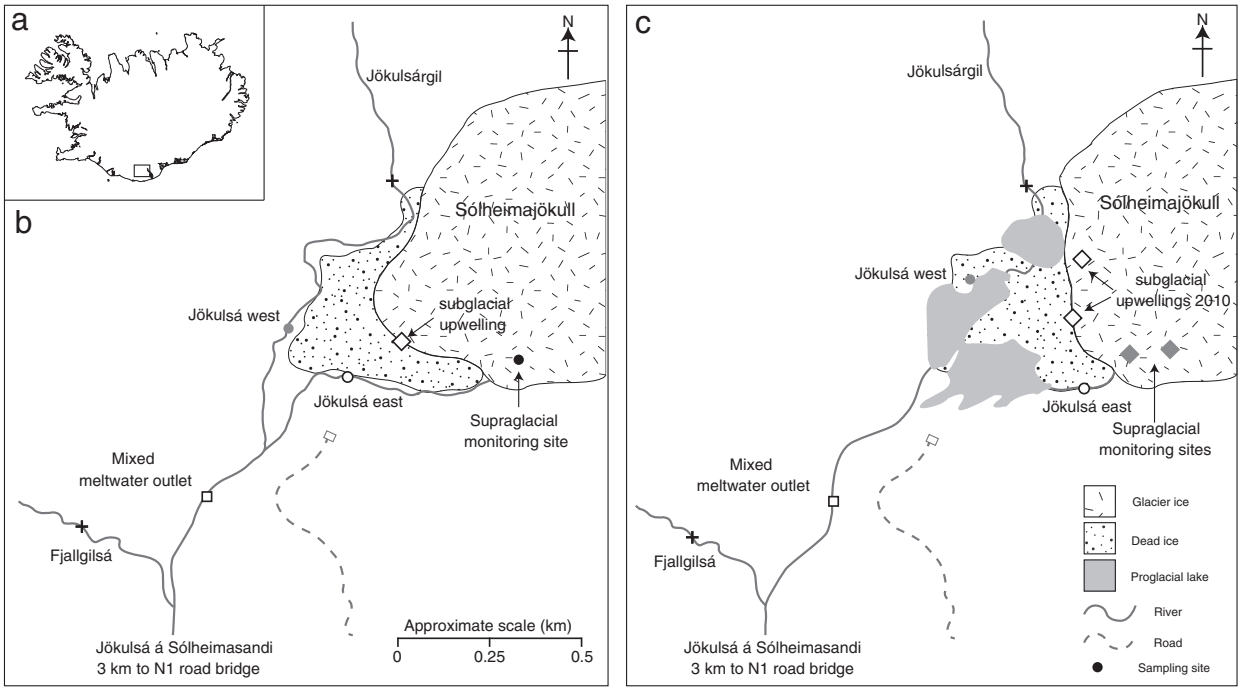

Fig. 1. Location map showing the Mýrdalsjökull ice cap and outlet glacier Sólheimajökull (panel a). The main sampling sites and proglacial drainage configuration during 2009–2010 are depicted in panel b and during 2012 in panel c.

Table 1
Sulphate concentrations, isotope values ($\delta^{34}S_{SO_4}$ and $\delta^{18}O_{SO_4}$, $\delta^{18}O/\delta^{2}H_{H_2O}$) and physico-chemical data for Sólheimajökull, during spring and summer field campaigns 2009–2012.

Year	Chemical species	Supraglacial	East	West	Mixed outlet	Bridge	Subglacial upwelling	External catchment inflow	Jökulsárgil Fjallgilsá
2009 (summer) day of year 204 to 210	$\delta^{34}S_{SO_4}$ (‰)	–	–	+5.1 (*n = 1*)	+3.1 (*n = 8*) (+2.6 to +3.4)	+4.7 (*n = 3*) (+4.5 to +4.9)	+3.0 (*n = 1*)	–	–
	$\delta^{18}O_{SO_4}$ (‰)	–	–	−0.3 (*n = 1*)	−3.9 (*n = 8*) (−6.0 to −3.3)	−1.1 (*n = 2*) (−2.0 to −0.3)	−5.2 (*n = 1*)	–	–
	$\delta^{18}O_{SO_4\ threshold}$ (‰)	–	–	−3.85 (*n = 1*)	−3.42 (*n = 8*) (−3.3 to −3.5)	−3.73 (*n = 2*) (−3.74 to −3.72)	−4.13 (*n = 1*)		
	SO_4 (mg/l)	0.19 (*n = 2*) (0.09 to 0.3)	2.58 (*n = 2*) (1.93 to 3.24)	3.85 (*n = 1*)	4.64 (*n = 9*) (3.87 to 5.86)	3.44 (*n = 4*) (2.92 to 4.18)	7.48 (n = 1)	–	–
	$\delta^{18}O_{H_2O}$ (‰)	−9.3 (*n = 2*) (−9.3 to −9.4)	−9.3 (*n = 2*) (−9.3 to −9.4)	−10.1 (*n = 1*)	−9.6 (*n = 9*) (−9.4 to −9.7)	−10.4 (*n = 4*) (−9.8 to −10.1)	−10.5 (*n = 1*)	–	–
	δD_{H_2O} (‰)	−63.1 (*n = 2*) (−63.1 to −63.2)	−62.8 (*n = 2*) (−62.8 to −62.9)	−67.9 (*n = 1*)	−64.8 (*n = 9*) (−63.7 to −66.0)	−66.3 (*n = 4*) (−65.3 to −67.9)	−70.6 (*n = 1*)	–	–
	pH	7.81 (*n = 2*) (7.27 to 8.34)	6.61 (*n = 2*) (6.60 to 6.62)	6.05 (*n = 1*)	6.58 (*n = 15*) (6.27 to 6.87)	6.55 (*n = 4*) (6.49 to 6.62)	6.05 (*n = 1*)	–	–
	Temperature (°C)	0.2 (*n = 2*) (0.1 to 0.2)	0.5 (*n = 2*) (0.4 to 0.6)	0.8 (*n = 1*)	1.8 (*n = 15*) (0.8 to 2.8)	2.1 (*n = 4*) (1.9 to 2.4)	0.1 (*n = 1*)	–	–
	EC (μS cm^{-1})	3 (*n = 2*) (2 to 4)	92.5 (*n = 2*) (89 to 96)	109 (*n = 1*)	104.5 (*n = 15*) (84 to 129)	97.5 (*n = 4*) (87 to 117)	171 (*n = 1*)	–	–
2010 (summer) day of year 200 to 209	$\delta^{34}S_{SO_4}$ (‰)	+0.9 (*n = 1*)	+2.4 (*n = 3*) (+1.8 to +2.9)	+2.2 (*n = 2*) (+1.5 to +2.8)	+2.2 (*n = 15*) (+1.6 to +2.8)	+2.8 (*n = 5*) (+2.1 to +3.2)	+1.5 (*n = 4*) (+0.9 to +1.9)	+3.0 (*n = 2*) (+2.8 to +3.1)	–
	$\delta^{18}O_{SO_4}$ (‰)	−1.41 (*n = 1*)	−4.01 (*n = 3*) (−3.99 to −4.03)	−3.82 (*n = 2*) (−5.4 to −2.2)	−4.34 (*n = 11*) (−4.8 to −2.4)	−2.84 (*n = 6*) (−3.1 to −2.3)	−5.42 (*n = 3*) (−4.0 to −6.4)	+0.08 (*n = 2*) (−0.2 to +0.3)	–
	$\delta^{18}O_{SO_4\ threshold}$ (‰)	−3.29 (*n = 1*)	−4.01 (*n = 3*) (−3.5 to −3.8)	−3.63 (*n = 2*) (−3.5 to −3.8)	−3.90 (*n = 15*) (−4.0 to −3.7)	−2.80 (*n = 5*) (−4.0 to −3.7)	−4.02 (*n = 3*) (−4.2 to −3.8)	−3.17 (*n = 2*) (−3.1 to −3.2)	–
	SO_4 (mg/l)	0.06 (*n = 6*) (0.04 to 0.12)	2.47 (*n = 4*) (2.38 to 2.58)	2.75 (*n = 2*) (2.44 to 3.06)	2.62 (*n = 22*) (2.25 to 3.08)	2.72 (*n = 8*) (2.24 to 2.99)	3.09 (*n = 13*) (1.88 to 6.09)	1.63 (*n = 2*) (1.57 to 1.69)	1.47 (*n = 1*)
	$\delta^{18}O_{H_2O}$ (‰)	−9.48 (*n = 6*) (−10.0 to −9.3)	−10 (*n = 4*) (−10.1 to −9.6)	−9.85 (*n = 2*) (−9.6 to −10.1)	−10.18 (*n = 22*) (−10.5 to −9.8)	−10.12 (*n = 8*) (−10.3 to −9.9)	−10.42 (*n = 13*) (−10.6 to −10.0)	−9.23 (*n = 2*) (−9.2 to −9.3)	−8.30 (*n = 1*)
	δD_{H_2O} (‰)	−62.47 (*n = 6*) (−66.8 to −59.5)	−67.48 (*n = 4*) (−68.1 to −66.2)	−66.35 (*n = 2*) (−66.8 to −65.9)	−67.87 (*n = 22*) (−70.0 to −64.5)	−67.94 (*n = 8*) (−67.2 to −69.2)	−68.77 (*n = 13*) (−70.7 to −67.2)	−62.47 (*n = 2*) (−62.5 to −62.4)	−55.07 (*n = 1*)
	$\delta^{34}S_{H_2S}$ (‰)	–	+5.8 (*n = 1*)	+5.9 (*n = 1*)	+5.9 (*n = 3*) (+5.8 to +6.2)	–	–	–	–
	pH	7.4 (*n = 6*) (7.15 to 7.91)	6.47 (*n = 4*) (5.99 to 6.80)	6.76 (*n = 2*) (6.76 to 6.76)	6.68 (*n = 21*) (6.46 to 7.16)	6.84 (*n = 8*) (6.62 to 7.07)	6.50 (*n = 13*) (6.2 to 7.34)	7.7 (*n = 2*) (7.56 to 7.84)	7.63 (*n = 1*)
	Temperature (°C)	0.12 (*n = 6*) (0.1 to 0.2)	0.3 (*n = 4*) (0.3 to 0.4)	2.15 (*n = 2*) (2.1 to 2.2)	1.00 (*n = 21*) (0.5 to 2.3)	1.91 (*n = 8*) (1.8 to 2.2)	0.3 (*n = 13*) (0.1 to 0.9)	2.3 (*n = 2*) (2.1 to 2.5)	5.2 (*n = 1*)
	EC (μS cm^{-1})	4.5 (*n = 6*) (2 to 9)	68.8 (*n = 4*) (64 to 73)	70.5 (*n = 2*) (64 to 77)	72.2 (*n = 21*) (61 to 84)	76.6 (*n = 8*) (69 to 88)	99.0 (*n = 13*) (59 to 213)	48 (*n = 2*) (46 to 50)	38 (*n = 1*)
	Dissolved oxygen (%)	102.7 (*n = 1*)	91.2 (*n = 4*) (87.0 to 98.8)	97.6 (*n = 2*) (96.1 to 99.1)	85.6 (*n = 14*) (44.2 to 103.4)	93.3 (*n = 7*) (66.4 to 103.3)	78.48 (*n = 13*) (65.1 to 88.1)	106.7 (*n = 1*)	103.5 (*n = 1*)
2012 (spring) day of year 108 to 121	$\delta^{34}S_{SO_4}$ (‰)	−0.6 (*n = 1*)	+2.8 (*n = 7*) (+2.2 to +3.3)	+4.4 (*n = 1*)	+5.0 (*n = 13*) (+4.2 to +5.3)	+5.5 (*n = 13*) (+5.0 to +5.8)	–	+5.2 (*n = 2*) (+4.8 to +5.7)	+7.7 (*n = 1*)
	$\delta^{18}O_{SO_4}$ (‰)	–	−1.65 (*n = 7*) (−1.9 to −1.4)	+0.66 (*n = 1*)	+0.26 (*n = 13*) (−0.4 to +1.2)	+1.02 (*n = 13*) (−0.1 to +2.8)	–	+2.56 (*n = 2*) (+1.8 to +3.4)	+5.60 (*n = 1*)
	$\delta^{18}O_{SO_4\ threshold}$ (‰)	–	−2.79 (*n = 7*) (−2.9 to −2.7)	−3.10 (*n = 1*)	−3.19 (*n = 13*) (−3.4 to −2.5)	−3.12 (*n = 13*) (−3.3 to −2.9)	–	−2.99 (*n = 2*) (−3.1 to −2.9)	−2.68 (*n = 1*)
	SO_4 (mg/l)	0.3 (*n = 2*) (0.28 to 0.36)	3.4 (*n = 7*) (2.58 to 4.2)	4.34 (*n = 1*)	5.3 (*n = 13*) (4.89 to 5.73)	4.6 (*n = 13*) (4.33 to 4.90)	–	4.0 (*n = 2*) (3.9 to 4.2)	2.64 (*n = 1*)
	$\delta^{18}O_{H_2O}$ (‰)	−9.13 (*n = 2*) (−9.14 to −9.11)	−8.71 (*n = 7*) (−8.9 to −8.6)	−9.13 (*n = 1*)	−9.25 (*n = 13*) (−9.5 to −8.4)	−9.15 (*n = 13*) (−9.4 to −8.8)	–	−8.99 (*n = 2*) (−9.1 to −8.9)	−8.57 (*n = 1*)
	δD_{H_2O} (‰)	−63.05 (*n = 2*) (−63.8 to −62.3)	−57.94 (*n = 7*) (−58.5 to −57.3)	−62.38 (*n = 1*)	−62.80 (*n = 10*) (−63.7 to −62.1)	−60.47 (*n = 13*) (−61.0 to −59.7)	–	−60.14 (*n = 2*) (−61.9 to −58.4)	−57.69 (*n = 1*)
	pH	7.0 (*n = 2*) (6.3 to 7.8)	8.8 (*n = 7*) (8.56 to 9.19)	7.1 (*n = 1*)	7.0 (*n = 13*) (6.17 to 7.35)	7.4 (*n = 13*) (6.88 to 8.33)	–	7.5 (*n = 2*) (7.50 to 7.56)	7.47 (*n = 1*)
	Temperature (°C)	(*n = 2*) –	0.1 (*n = 7*) (0.1 to 0.2)	2.4 (*n = 1*)	1.8 (*n = 13*) (1.0 to 3.4)	2.9 (*n = 13*) (1.9 to 4.1)	–	2.7 (*n = 2*) (2.7 to 2.7)	3.3 (*n = 1*)
	EC (μS cm^{-1})	8.5 (*n = 2*) (5 to 12)	76 (*n = 7*) (62 to 102)	143 (*n = 1*)	182.1 (*n = 13*) (165 to 200)	153 (*n = 13*) (138 to 162)	–	120.5 (*n = 2*) (118 to 123)	80 (*n = 1*)

= data unavailable. Values represent averages with *n* value provided. Data range provided in parentheses.

Table 2
Sulphate concentrations, isotope values ($\delta^{34}S_{SO_4}$ and $\delta^{18}O_{SO_4}$, $\delta^{18}O/\delta^{2}H_{H_2O}$) and physico-chemical data for Sólheimajökull, during September 2009–2012.

Chemical species at mixed outlet	$\delta^{34}S_{SO_4}$ (‰)	$\delta^{18}O_{SO_4}$ (‰)	$\delta^{18}O_{SO_4\ threshold}$ (‰)	SO_4 (mg/l)	pH	Temperature (°C)	EC (μS cm^{-1})
2009 (Sept) day of year 247	+1.44 *(n = 1)*	−3.87 *(n = 1)*	−3.42[a]	–	6.53	–	87
2010 (Sept) day of year 242	+0.01 *(n = 1)*	−8.52 *(n = 1)*	−3.88[a]	–	–	–	–
2011 (Sept) day of year 244	+1.87 *(n = 1)*	−5.3 *(n = 1)*	−3.65[b]	–	6.37	0.8	41
2012 (Sept) day of year 248	+3.2 *(n = 2)* (+3.7 to +2.7)	–	–	3.84 *(n = 2n)* (3.36 to 4.32)	–	–	–

[a] $\delta^{18}O_{SO_4\ threshold}$ has been calculated using $\delta^{18}O_{H_2O}$ values calculated as an average of the summer season mixed outlet.
[b] $\delta^{18}O_{SO_4\ threshold}$ has been calculated using $\delta^{18}O_{H_2O}$ values calculated as an average of the summer season mixed outlet from 2009 to 2010.

total volume of 1.5 ml and stored in micro-centrifuge tubes. Addition of 0.2 ml 1 M $BaCl_2$ solution to resin eluents enabled precipitation of sulphate as barium sulphate. Samples were allowed to crystallise for approximately 72 h under refrigeration prior to centrifugation and repeated washing. Product pellets of barium sulphate were oven dried before weighing into tin or silver capsules for $\delta^{34}S$ and $\delta^{18}O$ analysis respectively.

3.4. Mass spectrometric analysis

$^{34}S/^{32}S$ and $^{18}O/^{16}O$ ratios of product barium sulphate and zinc sulphide were determined by elemental analyser linked to a continuous flow isotope ratio mass spectrometer. Sulphur isotopes from samples collected during the 2009 field season, were analysed using a Thermo Flash EA linked to a Delta XP mass spectrometer at the NERC Isotope Geosciences Facility (NIGL). All other samples were analysed using an Elementar Pyrocube elemental analyser linked to an Isoprime 100 continuous flow mass spectrometer at the University of Lancaster. Combustion of samples within tin capsules in the presence of vanadium pentoxide at 1050 °C yielded SO_2 for determination of $\delta^{34}S_{SO_4}$ and pyrolysis within silver capsules in the presence of carbon black catalyst at 1450 °C yielded CO for determination of $\delta^{18}O_{SO_4}$. $\delta^{34}S$ values were corrected against VCDT using within run analyses of international standard NBS-127 and SO5 (assuming $\delta^{34}S$ values of +21.1‰ and +0.5‰ respectively and $\delta^{18}O$ was corrected to VSMOW using NBS-127 and SO6 (assuming $\delta^{18}O$ values of +9.3‰ and −11.3‰ respectively). Within-run standard replication (1 SD) was better than +/−0.3‰ for both sulphur and oxygen isotope values.

Water sample D/H and $^{18}O/^{16}O$ ratios were determined by continuous flow isotope ratio mass spectrometry at both the University of Lancaster (Elementar pyrocube elemental analyser linked to an Isoprime 100 mass spectrometer; datasets 2010–2012) and the University of Birmingham (Eurovector elemental analyser and multiflow linked to a GV Isoprime mass spectrometer; dataset 2009). For D/H determination, both analytical laboratories used sample injection aliquots of 0.3 μl followed by reduction to hydrogen at 1050 °C over chromium metal catalyst. $\delta^{18}O$ analyses at the University of Lancaster were undertaken in pyrolysis mode using sample injection of 0.4 μl over glassy carbon chips at 1450 °C. At the University of Birmingham, analysis was undertaken by equilibration with mixed headspace gas (95% He, 5% CO_2). δD and $\delta^{18}O$ values were corrected against laboratory calibration standards relative to V-SMOW and presented within the manuscript as non-normalised values. Within-run standard replication (1 SD) was better than +/−1‰ for δD in both laboratories. Standard replication for $\delta^{18}O$ was better than +/−0.4‰ and +/−0.1‰ for pyrolysis and equilibration techniques respectively.

4. Results

Sulphate concentrations, isotope values ($\delta^{34}S_{SO_4}$ and $\delta^{18}O_{SO_4}$, $\delta^{18}O/D_{H_2O}$) and physico-chemical data are compiled and presented within Tables 1 and 2. A plot of water isotope data (Fig. 2a) differentiates between supraglacial and subglacial meltwater sources during the summer season. However, this source distinction does not prevail during the spring season of 2012, where all water sources cluster tightly within the range dominated by water of supraglacial origin during summer (Fig. 2b). Isotope values presented in Table 1 demonstrate a range of $\delta^{34}S_{SO_4}$ between −0.8‰ and +7.7‰ with these end member values attributed to supraglacial meltwaters and stream waters originating from outside the catchment respectively. Dissolved hydrogen sulphide supports an isotopic composition ranging between +5.8 and +6.2‰ ($n = 5$) (Table 1). Bedrock from within the catchment does not contain measurable sulphur concentrations except for a pyrite bearing microcrystalline basalt (approximately 10% volume of rounded vesicles that are 1–4 mm across and partly filled with cubic pyrite crystals < 0.5 mm in length) found within a few key locations at the recently exposed ice margin and within samples of mixed subglacial till. The isotopic signature of this microcrystalline basalt (and mixed subglacial till) ranges between +0.1 and +1.6‰ ($n = 5$) and is capable of directly influencing subglacial waters which have undergone rock–water contact. A

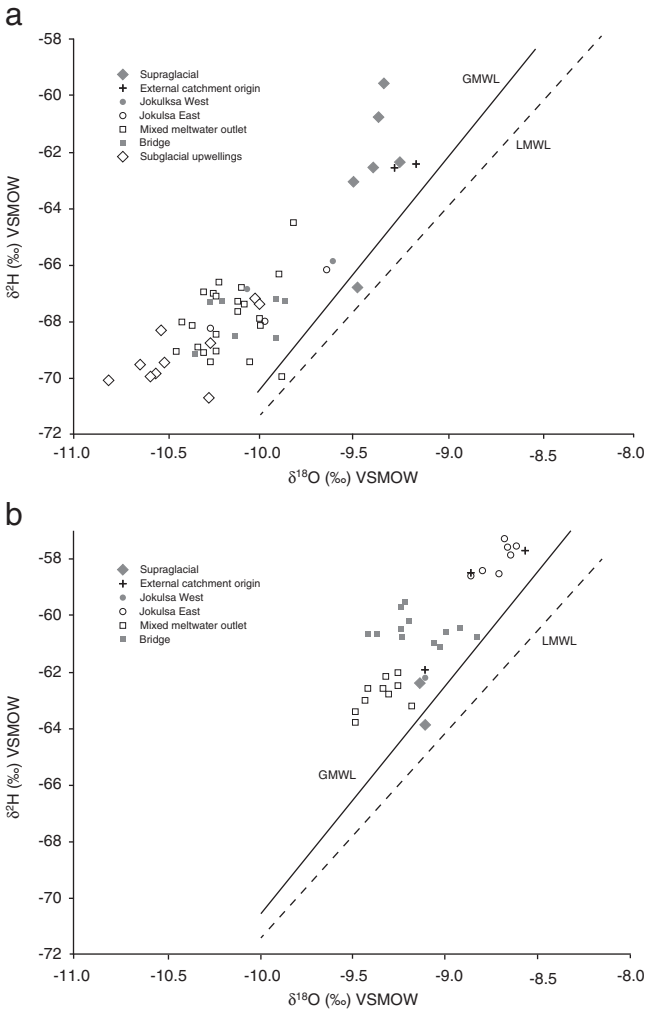

Fig. 2. Plot of $\delta^{18}O/D_{H_2O}$ for meltwater samples collected during summer 2010 (panel a) and Spring 2012 (panel b). The Global Meteoric Water Line (GMWL) is plotted as $\delta^{2}H = 8.17\ \delta^{18}O + 11.27$ (after Rozanski et al., 1993). The Local Meteoric Water Line (LMWL) is sourced from GNIP station Reykjavik (64° 07′ 48″, 21° 55′ 48″; 14 m.a.s.l.).

clear sample site distinction using both sulphur isotope values and concentrations is expressed as a mixing between supraglacial meltwaters, bedrock weathering and stream input of external catchment origin dependent upon seasonality (Fig. 3a,b). Oxygen isotopes within sulphate ($\delta^{18}O_{SO_4}$) range between −8‰ and +5.5‰, and lie either side of the threshold for depicting reducing/oxidising environments (Fig. 4a,b). A pronounced seasonality to the $\delta^{18}O_{SO_4}$ signatures depicts summer subglacial conditions, which are of a sub-oxic nature, and spring conditions which are fully oxidised.

5. Discussion

5.1. Seasonal evolution of the glacier drainage system

The hydrological evolution of Sólheimajökull operates in the fashion generally expected of any temperate glacier system. Discharge is at its lowest in the winter season due to a reduction in surface melting, although the volume of melt produced should be enough to retain open channel flow conditions in the lower portions of the ice mass. Above the winter snowline however, the snowpack thickens with altitude. Such conditions of snowpack storage limit the release of meltwaters to the glacier bed and subglacial hydrology existing beneath an ice mass with a deep snowpack can be expected to remain confined to linked cavity drainage, poorly connected to the channelized system existing at lower elevation (Fountain and Walder, 1998). Deuterium and oxygen isotopes of water would appear to support this hydrological configuration. Altitude has a fractionating effect upon isotopic signatures of $\delta^{18}O/D_{H_2O}$ such that values become depleted in ^{18}O and D as an air mass ascends to the upper reaches of the glacier (Arnason, 1977). This generates an offset from the Local Meteoric Water Line (LMWL) and an altitudinal range of isotopic values in the glacier surface snowpack. The presence of distinctive isotopic values for the supraglacial and subglacial water sources in Fig. 2a would suggest that the source waters originate from different altitudinal ranges. Supraglacial waters constitute some of the heaviest isotopic values on the local meteoric water line. Due to the crevassed nature of the glacier surface, supraglacial streams sampled in the lower reaches of the glacier are likely to be locally sourced and thereby originating from low elevation. The light isotopic end member on Fig. 2a is composed of upwelling waters of subglacial origin, likely representing snow/ice melt originating from higher elevation (cf. Griselin et al., 1994). During the spring season of 2012, this light isotopic end member is not apparent due to the absence of any subglacial upwelling waters and the glacier drainage system still being spatially restricted to the low elevations (Fig. 2b, Table 1). Enhanced summer season melting and headward expansion of drainage channels will subsequently re-establish a high volume subglacial drainage network penetrating beneath the accumulation zone and transporting meltwaters of high elevation origin.

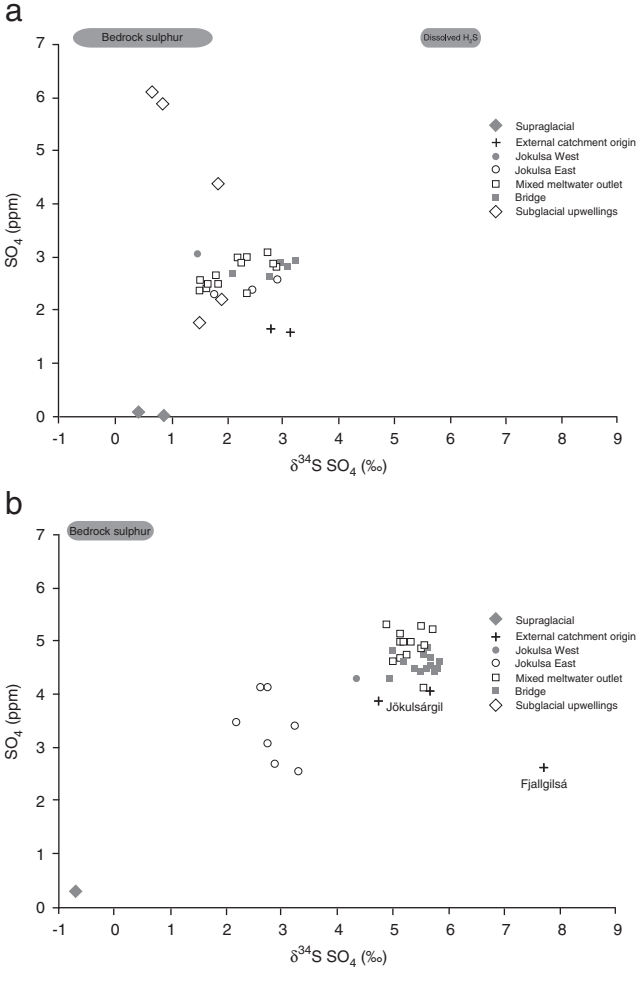

Fig. 3. $\delta^{34}S$ Vs $[SO_4]$ for sulphur sources and bulk meltwaters within the Sólheimajökull catchment. Data displayed are from summer 2010 (panel a) and Spring 2012 (panel b).

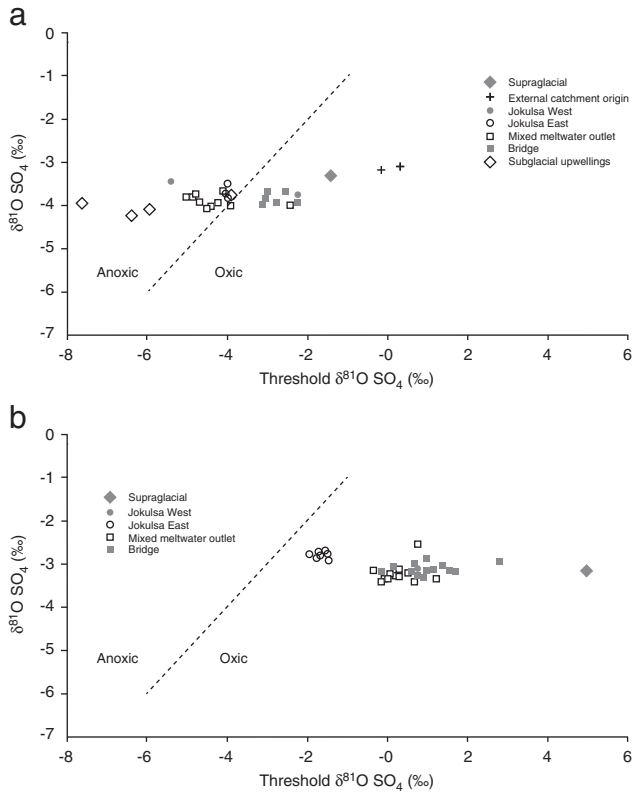

Fig. 4. $\delta^{18}O_{SO_4}$ Vs calculated threshold for oxidation of sulphide under reducing conditions. Threshold calculations are depicted through Eq. (3) (after Bottrell and Tranter, 2002). Data displayed are from summer 2010 (panel a) and spring 2012 (panel b).

5.2. Sources of sulphur in the Sólheimajökull system

Key sources of sulphur in the Sólheimajökull system during summer 2010 are depicted through Fig. 3a. Key inputs to the system consist of supraglacial meltwater, sulphur obtained from bedrock weathering, dissolved hydrogen sulphide and sulphur within streams that enter from outside the catchment. Mixing between these sources in variable proportion dominates the sulphur isotopic composition in the main meltwater streams.

Summer season supraglacial runoff from the glacier is necessarily low in sulphate concentration, reflecting the dilute nature of ice melt. The isotopic values are very similar to those found in the catchment bedrock (catchment bedrock = +0.1 to +1.6‰) and probably reflect either bedrock dust deposition and subsequent release through surface weathering, or dissolution of volcanic aerosol (~0‰ (Nielson, 1974)) attached to ash particulates deposited on the surface of the glacier (e.g. Flaathen and Gíslason, 2007; Olsson et al., 2013). Despite the close proximity of the ocean, there is little isotopic evidence for any marine input (~ +21‰ (Rees et al., 1978)). This contrasts markedly with the work of Gíslason and Torssander (2006) in which the main component of Icelandic winter precipitation is seen to be marine derived ($\delta^{34}S_{SO_4}$ = +13 to +19‰). This contrast is likely due to volcanic and bedrock sources detailed above being trapped during snowpack deposition, dominating the meltwater composition when released during melt. Streams originating from outside the catchment form another end-member to the mixing plot, forming some of the heaviest sulphur isotopic signatures (up to +7.7‰). These are likely obtained through contribution from soil and groundwater leachates during passage through high elevation pastures prior to entry into the Sólheimajökull catchment. The deposition of ash from the eruption of Eyjafjallajökull in May 2010 and its entrapment in surface vegetation is likely the cause of lighter isotopic values in streams of external catchment origin in summer 2010 compared to spring 2012. Further biogeochemical controls on the sulphur isotopic composition of waters emanating from vegetated soils include processes of assimilation (uptake) of sulphur into vegetation, re-mineralisation of organic matter, and long term storage of sulphur in both vegetation and soil. During processes of assimilation and mineralisation, a slight preference for incorporation of ^{32}S into the reaction products creates a fractionation of 1–2‰ (Krouse et al., 1991; Thode et al., 1991; Mitchell et al., 2001). Net uptake (assimilation) of sulphate by vegetation typically leaves soil sulphate solutions slightly enriched in ^{34}S (Zhang et al., 1998) and hence explains why the streams of external catchment origin form a sulphur isotopic end member enriched in ^{34}S relative to that released during snow and ice melt. Sulphur isotopic signatures obtained from the catchment bedrock match closely with those obtained from meltwaters of subglacial origin (sampled directly from upwelling zones), suggesting that bedrock weathering forms a third end-member to the system (Table 1 and Fig. 3a). Sulphur isotopic signatures collected from the bulk meltwater output (denoted 'mixed meltwater outlet' in Fig. 3) mainly plot between these three end member signatures, representing input from only three of the four possible sources. The fourth source (oxidation of dissolved hydrogen sulphide, $\delta^{34}S$ = +5.8 to +6.2‰) seems to hold only a weak influence over meltwater sulphate isotopic composition. Despite the fact that glacial meltwaters are previously recorded to contain concentrations of H_2S up to 3 ppm during the summer season (Sigvaldason, 1963; Lawler et al., 1996), this sulphur source does not seem to dominate the isotopic composition of the sulphate molecule. Optimal conditions promoting the oxidation of aqueous H_2S require pH 6.8–7.5. However, the meltwater pH of subglacial and bulk discharge is frequently below this value and a large proportion of residual oxygen is required to enable efficient oxidation (dissolved oxygen concentrations are typically below 100% during the summer season, Table 1). Rates of hydrogen sulphide oxidation are also limited by low temperatures. Environmental conditions are therefore not conducive to rapid oxidation of H_2S. Whilst conditions of <100% DO may be limiting to the oxidation of aqueous H_2S, oxidation of pyrite can proceed under sub-oxic conditions through the use of alternative oxidising agent FeIII under microbial catalysis (Eq. (2)), hence sulphate concentrations within the catchment meltwaters remain dominated by those obtained through mineral weathering and atmospheric deposition.

The chemical composition of subglacial water does not remain constant throughout the summer melt season but changes with subglacial hydrological evolution and source mixing. Subglacial waters periodically upwell along lines of structural weakness where ice is thin close to the margin (e.g. along remnants of thrust planes, and at the head of debris stripes), initially under pressure with high concentrations of sulphate and an isotopic composition similar to the surrounding bedrock. Sulphate content becomes more dilute with time (days) and isotopically similar to bulk meltwaters leaving the catchment (Fig. 3a). This evolution of $\delta^{34}S_{SO_4}$ likely represents initial drainage of isolated parts of the glacier bed, associated with increasing water pressures in distributed cavities. Subsequent chemical and isotopic dilution demonstrates mixing with other water sources (e.g. supraglacial recharge, stream waters originating from outside the catchment mixing beneath the floating dead ice area at the glacier snout) as the drainage system evolves. This is typical of the chemical switch depicted within Bottrell and Tranter (2002) and Wynn et al. (2006).

Samples collected for sulphur isotopic analysis at the road bridge, representing the outer limits of the sampled catchment approximately 5 km from the glacier snout, reside partly outside the mixing plot of Fig. 3a. This could be due to downstream oxidation of remaining hydrogen sulphide to sulphate, driven by stream turbulence and an increase in water temperature. On-going reactivity of suspended sediment and contributions from varying lithology throughout the catchment may also drive this subtle shift in isotopic composition. Alternatively, extra-glacial stream Fjallgilsá enters the main meltwater channel 3 km upstream from the bridge sampling site and has been shown in subsequent years to convey sulphate at lower concentrations, but enriched in ^{34}S compared to the main stream (Table 1). Either way, it is apparent that solute loads and isotopic determinations of sulphate undertaken at the edge of the catchment are not truly representative of processes occurring beneath the glacier and ice cap, but are associated with downstream mixing of water sources and geochemical evolution away from point of emergence from the subglacial environment.

In the absence of a subglacial water source in Spring 2012, bulk meltwater outputs are dominated by mixing between supraglacial meltwater and streams of external catchment origin (Fig. 3b). The Jökulsárgil water source of external catchment origin dominates the chemical composition of the mixed outlet sampling site, demonstrating the importance of this input as an end member of the Jökulsá á Sólheimasandi system in the spring season. A discernable evolution of the water composition to isotopic values slightly enriched in ^{34}S and of lesser sulphate concentration between the mixed outlet and bridge sampling site may be attributed to inputs from the Fjallgilsá stream, also of external catchment origin. It is possible that oxidation of small quantities of dissolved H_2S may also form an end member of the mixing plot, thereby accounting for enrichment in ^{34}S and increases in sulphate concentration. However, no detectable presence of H_2S, would preclude this possibility. Furthermore, the lack of a subglacial water source due to the restricted nature of the subglacial drainage system at this time of the year, is demonstrated through the restricted range in $\delta^{18}O_{H_2O}$ (Fig. 2b) and as such would prevent access to any subglacial source of H_2S.

5.3. Hydrological controls on subglacial geothermal volatile release

During the summer season, large portions of the glacier bed are drained by channels operating under atmospheric pressure. During times of minimal surface ablation (winter–spring), reduced meltwater discharge should dictate that large channels are squeezed closed through ice deformation and drainage becomes confined to linked cavities, which are comparatively isolated from any atmospheric source (Fountain and Walder, 1998). Commensurate with a switch in hydrological configuration, a change in the redox status of drainage pathways would also be expected. Under such a model, winter season subglacial conditions should be driven towards a reducing status as weathering reactions consume all available atmospheric gases, whilst summer season conditions are closer to fully oxidising.

However, subglacial redox status at Sólheimajökull appears inverse to this expected pattern, supported through signatures of sulphate–oxygen isotopes. During the summer season, the $\delta^{18}O_{SO_4}$ signature of

meltwaters which are at least partially sourced from the glacier bed, indicates the attainment of low redox status, calculated through Eq. (3) following Bottrell and Tranter (2002). Full reducing, closed system conditions (eg, Hartmann and Nielsen, 2012) and the activity of microbially mediated sulphate reduction are not in evidence as $\delta^{18}O_{SO_4}$ values are far from exchange equilibrium with water (Fritz et al., 1989). Fig. 4b demonstrates oxidising conditions during the winter season, indicative of a dominating influence from channelized subglacial flow conditions which are well-connected to the atmosphere and draining meltwaters from below the winter snowline. The presence of low redox conditions during the summer season is counter-intuitive to expectations of the hydrological system in operation and demands a mechanism of either removing oxygen from the system, or for a source of anoxic water to contribute to the meltwater discharge.

The conceptual model shown in Fig. 5 proposes a suite of controls determining the seasonal presence of meltwaters of low redox status. We propose that a combination of periodic increases in basal water pressure and summer season headward expansion of channelized drainage, enables connectivity to be established with a zone of subglacial geothermal activity beneath Mýrdalsjökull which discharges anoxic waters. The strength of this geothermal field is likely controlled through seasonal changes to the ice overburden pressure. Numerous cauldrons across the surface of Mýrdalsjökull, some of which reside within the Sólheimajökull catchment, provide surface expression of subglacial geothermal activity (Björnsson et al., 2000). High ice over-burden pressures and the inward-dipping ice surface topography at cauldrons would likely conspire to prevent continuous meltwater escape from the locale (Björnsson, 1988; Guðmundsson et al., 2004). Only when subglacial water pressures become great enough will ice over-burden pressures be exceeded and/or hydraulic fracturing enable the escape of anoxic water. The onset of the summer melt season has the effect of establishing seasonal hydraulic connectivity with the anoxic geothermal zone, thereby encouraging the release of confined geothermal meltwaters charged with reduced gases (including hydrogen sulphide). These waters travel through both subglacial cavities and channels and upwell at the glacier snout throughout the summer season (Fig. 5a). The reduction in water pressure during transition from high pressure linked cavities to low (atmospheric) pressure discrete channelized drainage will also encourage the degassing of H_2S initially emplaced under elevated overburden pressures. The limited oxygen content of the water drives bedrock sulphide oxidation utilising FeIII as an oxidising agent and dominates the chemical composition of the bulk meltwaters leaving the glacier catchment. The effects of bacterial disproportionation of sulphur intermediate compounds on the meltwater sulphate isotope content of meltwaters cannot be discounted (Böttcher et al., 2005), although the enrichment of $\delta^{18}O_{SO_4}$ compared to precursor water values is not great enough to unequivocally invoke this process. Low temperatures, low pH and below-saturated dissolved oxygen content (measured at the point of upwelling) all serve to minimise any oxidation of H_2S gas. A further possible effect of summer reductions in overburden pressure, due to the combination of summer snowmelt and the switch to a low-pressure subglacial drainage system, is to stimulate geothermal activity. It has been proposed that seasonal variations in snowpack thickness cause stress readjustments that favour eruptive activity in the summer/late summer months (Albino et al., 2010), consistent with preference for summer/late summer eruptions during historical activity at Katla (Thordarsson and Larsen, 2007). The Katla geothermal–volcanic system therefore appears highly sensitive to modest pressure changes (Albino et al., 2010). However, minimal change in the size of the surface cauldrons on a seasonal basis would suggest that the strength of geothermal activity is predominantly seasonally invariant, as increased summer geothermal activity would be expected to drive deepening of surface depressions (e.g. Guðmundsson et al., 2004). Evidence for anoxia is present in the samples collected in September of

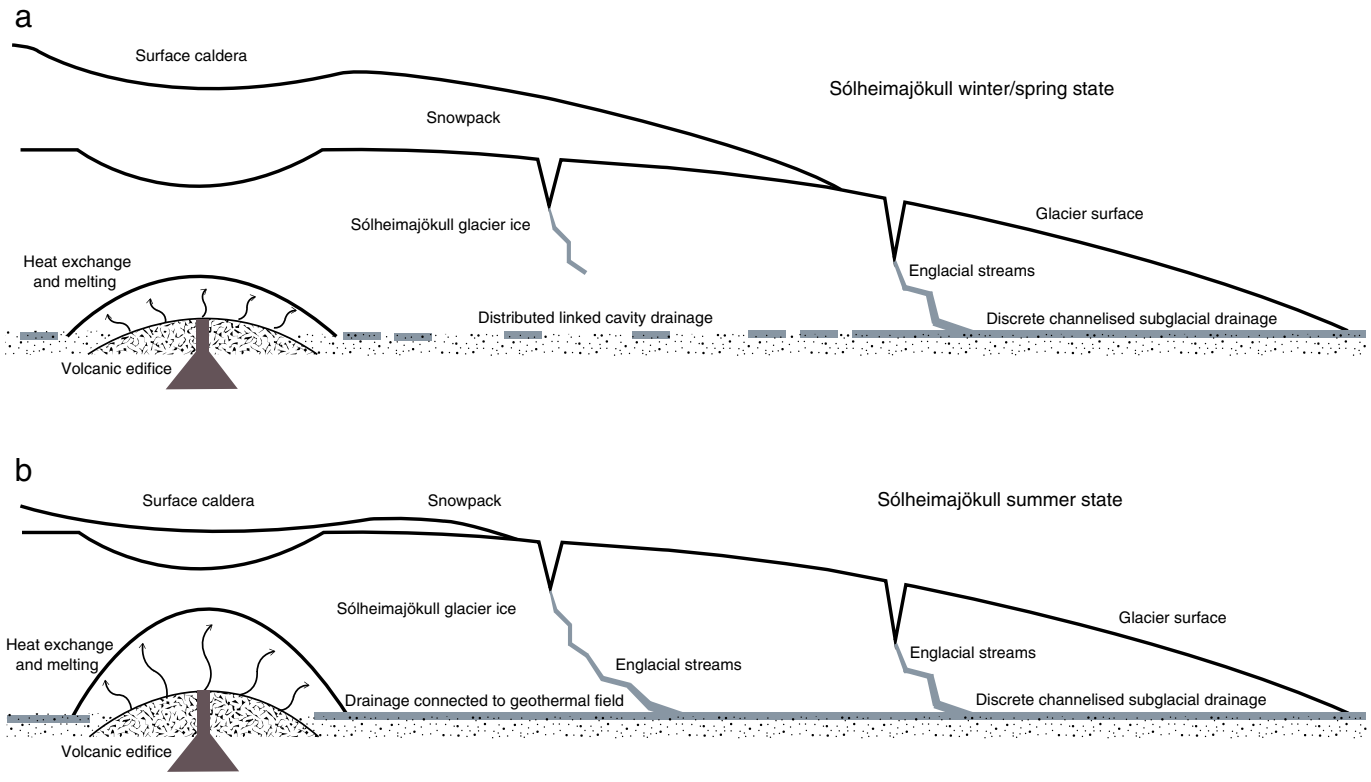

Fig. 5. Conceptual diagram showing the relationship between hydrological evolution and overburden pressure release leading to seasonality in meltwater geothermal indicators. Panel a) Spring season configuration showing discrete channelized subglacial hydrology limited to the lower portions of the glacier, a large ice and snow overburden pressure and limited connectivity to the zones of geothermal activity. Panel b) Summer season configuration depicting a well-developed channelized subglacial hydrological system which accesses the geothermal zone. Reduced overburden pressure enhances geothermal activity, heat exchange and volatile release.

each year (Table 2), sometime after which the commencement of high elevation snowfall and the restriction of the subglacial hydrological system to lower elevations will cut off the supply of anoxic geothermal water and fully oxic conditions will return (Fig. 5b). An alternative process capable of generating $\delta^{18}O_{SO_4}$ values close to those of $\delta^{18}O_{H_2O}$, involves high rates of oxygen isotopic exchange between sulphate molecules and surrounding water under conditions of high temperature and low pH (Lloyd, 1968). However, geothermal sulphur sources hold only a weak influence over isotopic signatures of sulphate (Fig. 3a) and it is likely that temperatures of melt waters at the ice–bed interface will not be high enough to promote oxygen isotopic exchange between water and sulphate obtained through bedrock weathering. Therefore, in our conceptual model (Fig. 5) the geochemical signature of meltwater is predominantly driven by hydrological reconfiguration. Only when the subglacial drainage system expands to connect with geothermal areas, do sulphate isotopes form sensitive indicators of subglacial geothermal activity through redox status imprinted in the sulphate molecule. Seasonal reconfiguration of meltwater drainage above the Katla geothermal field, may create shifting abundance and pressure of meltwater at the glacier base. This could also drive seasonal patterns of shallow low-frequency seismicity and pressure that encourage seismogenic slip at the ice–bedrock boundary in summer months (Jonsdottir et al., 2007, 2009).

6. Conclusions

Stable isotopes of sulphate and sulphide have been used with the ultimate aim of establishing a geochemical fingerprint of subglacial geothermal activity beneath the Mýrdalsjökull ice cap. The ubiquitous nature of sulphate in most glacial meltwaters and the expectation for rapid oxidation of reduced sulphurous gases, make the sulphate molecule an attractive contender as an indicator of subglacial geothermal processes. However, sulphur isotopes demonstrate that sulphate in the bulk meltwaters leaving the Sólheimajökull catchment can be accounted for through a three way mixing of sources, including oxidation of bedrock sulphides, supraglacial melt and stream water inputs of external catchment origin. Aqueous hydrogen sulphide, suspected to be of geothermal provenance does not appear to be readily oxidised to sulphate due to sub-optimal environmental conditions of pH, temperature and dissolved oxygen content. Sulphate and aqueous sulphide thereby remain two separate components of the sulphur biogeochemical cycle. However, oxygen isotopes within the sulphate molecule provide a strong sense of redox status, which demonstrate seasonal variation opposite to that expected in alpine and arctic glaciers which do not reside over a geothermal field. At Sólheimajökull, anoxic conditions prevail during the summer when drainage systems are fully developed and would normally be expected to convey waters under fully oxygenated conditions, suggesting a substantial input of reduced gases of geothermal origin. Under winter conditions, the waters are fully oxygenated suggesting limited geothermal contribution and an open hydrological system resulting from year round melting on the lower portions of the glacier. Seasonality of the $\delta^{18}O_{SO_4}$ geochemical fingerprint is considered the result of a strong summer geothermal contribution associated with subglacial drainage reconfiguration, and unloading due to surface melting. This is also likely closely linked with the seasonal patterns of shallow seismicity detected at Katla, and the tendency for geothermal events and eruptions to occur during the summer months. Oxygen isotopes of sulphate are thereby deemed to provide a sensitive indicator of subglacial processes, recording shifts in hydrological connectivity at a large geothermal system that is entirely obscured by ice. Further development of this conceptual model is now required in order to build a better understanding of the role of the overlying ice mass upon mediating subglacial geothermal activity and the controls exerted upon the release of dissolved volatiles through meltwater streams.

Acknowledgements

This work was supported through University of Lancaster funding initiatives and research support to D. Morrell. H Tuffen is supported by a Royal Society University Research Fellowship. Isotope analysis was undertaken at the NERC Isotope Geosciences Laboratories, the University of Birmingham, and the University of Lancaster stable isotope facility. Thanks are expressed to D. Hughes for isotope analysis and method development, and to M. Auladell-Mestre for field support and laboratory analysis. We are grateful for the permissions granted from the Icelandic authorities to undertake this work, and especially to land owner Tómas Ísleiffsson for allowing access to the field site.

References

Albino, F., Pinel, V., Sigmundsson, F., 2010. Influence of surface load variations on eruption likelihood: application to two Icelandic subglacial volcanoes, Grímsvötn and Katla. Geophys. J. Int. 181, 1510–1524.
Arnason, B., 1977. Hydrothermal systems in Iceland traced by deuterium. Geothermics 5, 125–151.
Barkan, E., Luz, B., 2005. High precision measurements of $^{17}O/^{16}O$ and $^{18}O/^{16}O$ ratios in H_2O. Rapid Commun. Mass Spectrom. 19 (24), 3737–3742.
Bell, R.E., 2008. The role of subglacial water in ice-sheet mass balance. Nat. Geosci. http://dx.doi.org/10.1038/ngeo186.
Björnsson, H., 1988. Hydrology of Ice Caps in Volcanic Regions. Societas Scientiarum Islandica, 45, Reykjavikpp. 1–139.
Björnsson, H., Pálsson, F., Guðmundsson, M.T., 2000. Surface and bedrock topography of the Mýrdalsjökull ice cap, Iceland: the Katla caldera, eruption sites and routes of jökulhlaups. Jökull 49, 29–46.
Böttcher, M.E., Thamdrup, B., 2001. Anaerobic sulphide oxidation and stable isotope fractionation associated with bacterial sulphur disproportionation in the presence of MnO_2. Geochim. Cosmochim. Acta 65 (10), 1573–1581.
Böttcher, M.E., Thamdrup, B., Vennemann, T.W., 2001. Oxygen and sulphur isotope fractionation during anaerobic bacterial disproportionation of elemental sulphur. Geochim. Cosmochim. Acta 65 (10), 1601–1609.
Böttcher, M.E., Thamdrup, B., Gehre, M., Theune, A., 2005. $^{34}S/^{32}S$ and $^{18}O/^{16}O$ fractionation during sulphur disproportionation by *Desulfobulbus propionicus*. Geomicrobiol J. 22, 219–226.
Bottrell, S.H., Tranter, M., 2002. Sulphide oxidation under partly anoxic conditions at the bed of Haut Glacier D'Arolla, Switzerland. Hydrol. Process. 16 (5), 959–993.
Brown, G.H., Sharp, M.J., Tranter, M., Gurnell, A.M., Nienow, P.W., 1994. Impact of post mixing chemical reactions on the major ion chemistry of bulk meltwaters draining the Haut Glacier D'Arolla, Vallais, Switzerland. Hydrol. Process. 8, 465–480.
Canfield, D.E., Thamdrup, B., 1994. The production of ^{34}S-depleted sulphide during bacterial disproportionation of elemental sulfur. Science 266, 1973–1975.
Carswell, D.A., 1983. The volcanic rocks of the Sólheimajökull area, southern Iceland. Jökull 33, 61–71.
Cooper, R.J., Wadham, J.L., Tranter, M.J., Hodgkins, R., Peters, N.E., 2002. Groundwater hydrochemistry in the active layer of the proglacial zone, Finsterwalderbreen, Svalbard. J. Hydrol. 269, 208–223.
Dugmore, A.J., Sugden, D.E., 1991. Do the anomalous fluctuations of Sólheimajökull reflect ice-divide migration? Boreas 20, 105–113.
Duller, R.A., Mountney, N.P., Russell, A.J., Cassidy, N.C., 2012. Architectural analysis of a volcaniclastic jökulhlaup deposit, southern Iceland: sedimentary evidence for supercritical flow. Sedimentology 55, 939–964.
Elefsen, S.O., Snorrason, A., Haraldsson, H., Gíslason, S., Kristmannsdóttir, H., 2002. Real time monitoring of glacial rivers in Iceland. In: Snorrason, A., Finnsdóttir, H.P., Moss, M. (Eds.), The Extremes of the Extremes: Extraordinary Floods. Proceedings of a Reykjavik Symposium. IAHS Publ no. 271, pp. 199–204.
Fairchild, I.J., Killawee, J.A., Sharp, M.J., Spiro, B., Hubbard, B., Lorrain, R.D., Tison, J.L., 1999. Solute generation and transfer from a chemically reactive alpine–proglacial system. Earth Surf. Process. Landf. 24, 1189–1211.
Flaathen, T.K., Gíslason, S.R., 2007. The effect of volcanic eruptions on the chemistry of surface waters: the 1991 and 2000 eruptions of Mt. Hekla, Iceland. J. Volcanol. Geotherm. Res. 164 (4), 293–316.
Flowers, G.E., Björnsson, H., Pálsson, F., 2003. New insights into the subglacial and periglacial hydrology of Vatnajökull, Iceland, from a distributed physical model. J. Glaciol. 49 (165), 257–270.
Fountain, A.G., Walder, J., 1998. Water flow through temperate glaciers. Rev. Geophys. 36, 299–328.
Fritz, P., Basharmal, G.M., Drimmie, R.J., Ibsen, J., Qureshi, R.M., 1989. Oxygen isotope exchange between sulphate and water during bacterial reduction of sulphate. Chem. Geol. Isot. Geosci. 79, 99–105.
Galeczka, I., Oelkers, E.H., Gíslason, S.R., 2014. The chemistry and element fluxes of the July 2011 Múlakvísl and Kaldakvísl glacial floods, Iceland. J. Volcanol. Geotherm. Res. 273, 41–57.
Gíslason, S.R., Torssander, P., 2006. Response of sulphate concentration and isotope composition in Icelandic rivers to the decline in global atmospheric SO_2 emissions into the North Atlantic region. Environ. Sci. Technol. 40, 680–686.
Gíslason, S.R., Snorrason, A., Kristmannsdottir, H., Sveinbjörnsdóttir, Á.E., Torsander, P., Ólafsson, J., Castet, S., Dupré, B., 2002. Effects of volcanic eruptions on the CO_2 content

of the atmosphere and the oceans: the 1996 eruption and flood within the Vatnajökull Glacier, Iceland. Chem. Geol. 190, 181–205.
Griselin, M., Marlin, C., Dever, L., Moreau, L., 1994. Hydrology and geochemistry of the Loven East glacier, Spitsbergen. In: Griselin, M. (Ed.), Actes du 3e symposium international Cavités glaciers et cryokarst en regions polaires et de haute montagne, Chamonix-France. Annales littéraires de l'université de Besançon n° 561. série Géographie n°34, pp. 61–76.
Guðmundsson, M.T., Sigmundsson, F. Björnsson H., Högnadóttir, T., 2004. The 1996 eruption at Gjálp, Vatnajökull ice cap, Iceland: efficiency of heat transfer, ice deformation and subglacial water pressure. Bull. Volcanol. 66, 46–65.
Guðmundsson, M.T., Hoganadottir, P., Kristinsson, A.B., Gudbjornsson, S., 2007. Geothermal activity in the subglacial Katla caldera, Iceland, 1999–2005, studied with radar altimetry. Ann. Glaciol. 45, 66–72.
Guðmundsson, M.T., Larsen, G., Höskuldsson, Á., Gylfason, Á.G., 2008. Volcanic hazards in Iceland. Jökull 58, 251–268.
Hákonarson, M., 1860. (19th July) Kötluhlaup i Jökulsá á Sólheimasandi. Íslendingur 1.
Hartmann, M., Nielsen, H., 2012. $\delta^{34}S$ values in recent sea sediments and their significance using several sediment profiles from the western Baltic sea. Isot. Environ. Health Stud. 48 (1), 7–32.
Hodson, A.J., Mumford, P.N., Kohler, J., Wynn, P.M., 2005. The High Arctic glacial ecosystem: new insights from nutrient budgets. Biogeochemistry 72, 233–256.
Holt, B.D., Kumar, R., 1991. Oxygen isotope fractionation for understanding the sulphur cycle. In: Stable isotopes: natural and anthropogenic sulphur in the environment. In: Krouse, H.R., Grinenko, V.A. (Eds.), SCOPE 43. Wiley, New York, pp. 27–41.
Huybers, P., Langmuir, C., 2009. Feedback between deglaciation, volcanism and atmospheric CO_2. Earth Planet. Sci. Lett. 286, 479–491.
Irvine-Fynn, T.D.L., Hodson, A.J., 2010. Biogeochemistry and dissolved oxygen dynamics at a subglacial upwelling, Midtre Lovénbreen, Svalbard. Ann. Glaciol. 51 (56), 41–46.
Jenkins, K.A., Bao, H., 2006. Multiple oxygen and sulphur isotope compositions of atmospheric sulphate in Baton Rouge, LA, USA. Atmos. Environ. 40, 4528–4537.
Jonsdottir, K., Tryggvason, A., Roberts, R., et al., 2007. Habits of a glacier-covered volcano: seismicity patterns and velocity structure of Katla volcano, Iceland. Ann. Glaciol. 45, 169–177.
Jonsdottir, K., Roberts, R., Pohjola, V., Lund, B., 2009. Glacial long period seismic events at Katla volcano, Iceland. Geophys. Res. Lett. 36 (art no. L11402.).
Jonsell, U., Hansell, M., Mörth, C., Torssander, P., 2005. Sulfur isotopic signals in two shallow ice cores from Dronning Maud land, Antarctica. Tellus B 57 (4), 341–350.
Kamb, B., 1987. Glacier surge mechanism based on linked cavity configuration of the basal water conduit system. J. Geophys. Res. 92, 9083–9100.
Kristmannsdóttir, H., Gíslason, S., Haraldsson, H., Hauksdóttir, S., Gunnarsson, A., 2002. Seasonal variation in the chemistry of glacial-fed rivers in Iceland. In: Snorrason, A., Finnsdóttir, H.P., Moss, M. (Eds.), The Extremes of the Extremes: Extraordinary Floods. Proceedings of a Reykjavik Symposium, IAHS Publ no. 271, pp. 223–229.
Krouse, H.R., Stewart, J.W.B., Grinenko, V.A., 1991. Pedosphere and biosphere. In: Krouse, H.R., Grinenko, V.A. (Eds.), Stable Isotopes in the Assessment of Natural and Anthropogenic Sulphur in the Environment. SCOPE. John Wiley and Sons, Ltd, pp. 267–306.
Kruger, J., Schomacker, A., Benediktsson, I.O., 2010. Ice-marginal environments: geomorphic and structural genesis of marginal moraines at Mýrdalsjökull. In: Schmacker, A., Kruger, J., Kjaer, K.H. (Eds.), The Mýrdalsjökull Ice Cap, Iceland, 13 ed. Elsevier, Amsterdam.
Larsen, G., 2010. Katla: tephrochronology and eruption history. In: Schmacker, A., Kruger, J., Kjaer, K.H. (Eds.), The Mýrdalsjökull Ice Cap, Iceland, 13 ed. Elsevier, Amsterdam.
Larsen, G., Newton, A.J., Dugmore, A.J., Vilmundardottir, E.G., 2001. Geochemistry, dispersal, volumes and chronology of Holocene silicic tephra layers from the Katla volcanic system, Iceland. J. Quat. Sci. 16, 119–132.
Lawler, D., Björnsson, H., Dolan, M., 1996. Impact of subglacial geothermal activity on meltwater quality in the Jökulsá á Sólheimasandi system, southern Iceland. Hydrol. Process. 10, 557–577.
Le Heron, D.P., Etienne, J.L., 2005. A complex subglacial clastic dyke swarm, Sólheimajökull, southern Iceland. Sediment. Geol. 181, 25–37.
Lliboutry, L.L., 1968. General theory of subglacial cavitation and sliding of temperate glaciers. J. Glaciol. 7, 21–58.
Lliboutry, L.L., 1979. Local friction laws for glaciers: a critical review and new openings. J. Glaciol. 23, 67–95.
Lloyd, R.M., 1968. Oxygen isotope behaviour in the sulphate–water system. J. Geophys. Res. 73, 6099–6110.
Mackintosh, A.N., Dugmore, A.J., Hubbard, A.L., 2002. Holocene climatic changes in Iceland: evidence from modelling glacier length fluctuations at Sólheimajökull. Quat. Int. 91, 39–52.
Mayer, B., 1998. Potential and limitations of using sulphur isotope abundance ratios as an indicator for natural and anthropogenic induced environmental change. Isotope Techniques in the Study of Environmental Change. Proceedings of an International Conference in Vienna, Austria, pp. 423–435 (IAEA, Vienna Austria, 14–18th April 1997).
Mitchell, M.J., Mayer, B., Bailey, S.W., Hornbeck, J.W., Alewell, C., Driscoll, C.T., Likens, G.E., 2001. Use of stable isotope ratios for evaluating sulphur sources and losses at the Hubbard Brook experimental forest. Water Air Soil Pollut. 130, 75–86.
Newman, L., Krouse, H.R., Grinenko, V.A., 1991. Stable isotopes: natural and anthropogenic sulphur in the environment. In: Krouse, H.R., Grinenko, V.A. (Eds.), SCOPE 43. Wiley, New York, pp. 27–41.
Nielsen, H., Pilot, J., Grinenko, L.N., Lein, Y., Smith, J.W., Pankina, And, Pankina, R.G., 1991. Stable isotopes: natural and anthropogenic sulphur in the environment. In: Krouse, H.R., GrinenkO, V.A. (Eds.), SCOPE 43. Wiley, New York, pp. 27–41.
Nielson, H., 1974. Isotopic composition of the major contributors to atmospheric sulphur. Tellus, XXVI 211–221.
Ohmoto, H., Rye, R.O., 1979. Isotopes of sulphur and carbon. In: Barnes, H.L. (Ed.), Geochemistry of Hydrothermal Ore Deposits. Wiley, New York, pp. 509–567.
Olsson, J., Stipp, S.L.S., Dalby, K.N., Gíslason, S.R., 2013. Rapid release of metal salts and nutrients from the 2011 Grímsvötn, Iceland volcanic ash. Geochim. Cosmochim. Acta 123, 134–149.
Pagli, C., Sigmundsson, F., 2008. Will present day glacier retreat increase volcanic activity? Stress induced by recent glacier retreat and its effect on magmatism at the Vatnajökull ice cap, Iceland. Geophys. Res. Lett. 35 (Art. No L09304).
Patris, N., Delmas, R.J., Jouzel, J., 2000. Isotopic signatures of sulphur in shallow Antarctic ice cores. J. Geophys. Res. 105 (D6), 7071–7078.
Rees, C.E., Jenkins, W.J., Monster, J., 1978. The sulphur isotopic composition of ocean water sulphate. Geochim. Cosmochim. Acta 42 (4), 377–381.
Roberts, M.J., Russell, A.J., Tweed, F.S., Knudsen, Ó., 2000. Ice fracturing during jökulhlaups: implications for englacial floodwater routing and outlet development. Earth Surf. Process. Landf. 25, 1429–1446.
Roberts, M.J., Tweed, F.S., Russell, A.J., Knudsen, Ó., Harris, T.D., 2003. Hydrologic and geomorphic effects of temporary ice-dammed lake formation during jökulhlaups. Earth Surf. Process. Landf. 28, 723–737.
Robinson, Z.P., Fairchild, I.J., Spiro, B., 2009. The sulphur isotope and hydrochemical characteristics of Skeiðarársandur, Iceland: identification of solute sources and implications for weathering processes. Hydrol. Process. 23, 2212–2224.
Rozanski, K., Araguás-Araguás, L., Gonfiantini, R., 1993. Isotopic patterns in modern global precipitation. Continental Isotope Indicators of Climate, American Geophysical Union Monograph.
Russell, A.J., Tweed, F.S., Roberts, M.J., Harris, T.D., Guðmundsson, M.T., Knudsen, Ó., Marren, P.M., 2010. An unusual jökulhlaup resulting from subglacial volcanism, Sólheimajökull, Iceland. Quat. Sci. Rev. 29, 1363–1381.
Scharrer, K., Spieler, O., Mayer, C., Münzer, U., 2008. Imprints of sub-glacial volcanic activity on a glacier surface—SAR study of Katla volcano, Iceland. Bull. Volcanol. 70, 495–506.
Schomacker, A., Benediktsson, Í.Ö., Ingólfsson, Ó., Friis, B., Korsgaard, N.J., Kjær, K.H., Keiding, J.K., 2012. Late Holocene and modern glacier changes in the marginal zone of Sólheimajökull, South Iceland. Jökull 62, 111–130.
Sigurdsson, O., 2010. Variations of Mýrdalsjökull during postglacial and historic times. In: Schmacker, A., Kruger, J., Kjaer, K.H. (Eds.), The Mýrdalsjökull Ice Cap, Iceland, 13 ed. Elsevier, Amsterdam.
Sigvaldason, G.E., 1963. Influence of geothermal activity on the chemistry of three glacier rivers in southern Iceland. Jökull 13.
Spence, M.J., Bottrell, S.H., Thornton, S.F., Lerner, D.N., 2001. Isotopic modelling of the significance of sulphate reduction for phenol attenuation in a polluted aquifer. J. Contam. Hydrol. 53, 285–304.
Staines, K.E., Carrivick, J.L., Tweed, F.S., Evans, A.E., Russell, A.J., Jóhannesson, T., Roberts, M., 2014. A multi-dimensional analysis of proglacial landscape change at Sólheimajökull, southern Iceland. Earth Surface Processes and Landforms (in press).
Strebel, O., Böttcher, J., Fritz, P., 1990. Use of isotope fractionation of sulfate–sulfur and sulfate–oxygen to assess bacterial desulfurication in a sandy aquifer. J. Hydrol. 121, 155–172.
Sturkell, E., Einarsson, P., Sigmundsson, F., Hooper, A., Ofeigsson, B.G., Geirsson, H., Olafsson, H., 2010. Katla and Eyjafjallajökull Volcanoes. In: Schomacker, A., Kruger, J., Kjaer, K.H. (Eds.), The Mýrdalsjökull Ice Cap, Iceland, 13 ed. Elsevier, Amsterdam.
Taylor, B.E., Wheeler, M.C., Nordstrom, D.K., 1984. Isotope composition of sulphate in acid mine drainage as a measure of bacterial oxidation. Nature 308, 538–541.
Thode, H.G., 1991. Sulphur isotopes in nature and the environment: an overview. In: Krouse, H.R., Grinenko, V.A. (Eds.), Stable Isotopes in the Assessment of Natural and Anthropogenic Sulphur in the Environment. SCOPE. John Wiley and Sons, Ltd, pp. 267–306.
Thorarinsson, S., 1939. The ice-dammed lakes of Iceland, with particular reference to their value as indicators of glacier oscillations. Geogr. Ann. 21, 216–242.
Thordarsson, T., Larsen, G., 2007. Volcanism in Iceland in historical time: volcano types, eruption styles and eruptive history. J. Geodyn. 43 (1), 118–152.
Torssander, P., 1988. Sulfur isotope ratios of Icelandic lava incrustations and volcanic gas. J. Volcanol. Geotherm. Res. 35, 227–235.
Torssander, P., 1989. Sulfur isotope ratios of Icelandic rocks. Contrib. Mineral. Petrol. 102 (1), 18–23.
Tranter, M., Brown, G., Raiswell, R., Sharp, M., Gurnell, A., 1993. A conceptual model of solute acquisition by Alpine glacial meltwaters. J. Glaciol. 39 (133), 573–581.
Tranter, M., Sharp, M.J., Brown, G.H., Willis, I.C., Hubbard, B.P., Nielson, M.K., Smart, C.C., Gordon, S., Tulley, M., Lamb, H.R., 1997. Variability in the chemical composition of *in situ* subglacial meltwaters. Hydrol. Process. 11, 59–77.
Tuffen, H., 2010. How will melting of ice affect volcanic hazards in the twenty-first century? Phil. Trans. R. Soc. A 368, 2535–2558.
Wadham, J.L., Bottrell, S., Tranter, M., Raiswell, R., 2004. Stable isotope evidence for microbial sulphate reduction at the bed of a polythermal high Arctic glacier. Earth Planet. Sci. Lett. 219, 341–355.
Wadham, J.L., Cooper, R.J., Tranter, M., Bottrell, S., 2007. Evidence for widespread anoxia in the proglacial zone of an Arctic glacier. Chem. Geol. 243, 1–15.
Walder, J.S., 1986. Hydraulics of subglacial cavities. J. Glaciol. 32, 439–445.
Wynn, P.M., Hodson, A.J., Heaton, T.H.E., 2006. Chemical and isotopic switching within the subglacial environment of a high Arctic polythermal glacier. Biogeochemistry 78, 173–193.
Wynn, P.M., Hodson, A.J., Heaton, T.H.E., Chenery, S., 2007. Nitrate production beneath a High Arctic Glacier. Chem. Geol. 244, 88–102.
Zhang, Y., Mitchell, M.J., CFhrist, M., Likens, G.E., Krouse, R.H., 1998. Stable sulphur isotopic biogeochemistry of the Hubbard Brook Experimental Forest, New Hampshire. Biogeochemistry 41, 259–275.